

# AAV-mediated Gene Delivery in Dp71-null Mouse Model with Compromised Barriers

Ophélie Vacca,<sup>1</sup> Marie Darche,<sup>1</sup> David V. Schaffer,<sup>2</sup> John G. Flannery,<sup>3</sup>  
José-Alain Sahel,<sup>1,4,5,6</sup> Alvaro Rendon,<sup>1</sup> and Deniz Dalkara<sup>1</sup>

Formation and maintenance of the blood–retinal barrier (BRB) is required for proper vision and breaching of this barrier contributes to the pathology in a wide variety of retinal conditions such as retinal detachment and diabetic retinopathy. Dystrophin Dp71 being a key membrane cytoskeletal protein, expressed mainly in Müller cells, its absence has been related to BRB permeability through delocalization and down-regulation of the AQP4 and Kir4.1 channels. Dp71-null mouse is thus an excellent model to approach the study of retinal pathologies showing blood–retinal barrier permeability. We aimed to investigate the participation of Müller cells in the BRB and in the inner limiting membrane of Dp71-null mice compared with wild-type mice in order to understand how these barriers work in this model of permeable BRB. To this aim, we used an Adeno-associated virus (AAV) variant, ShH10-GFP, engineered to target Müller cells specifically. ShH10 coding GFP was introduced by intravitreal injection and Müller cell transduction was studied in Dp71-null mice in comparison to wild-type animals. We show that Müller cell transduction follows a significantly different pattern in Dp71-null mice indicating changes in viral cell-surface receptors as well as differences in the permeability of the inner limiting membrane in this mouse line. However, the compromised BRB of the Dp71-null mice does not lead to virus leakage into the bloodstream when the virus is injected intravitreally – an important consideration for AAV-mediated retinal gene therapy.

GLIA 2013;00:000–000

**Key words:** Dystrophin Dp71, Müller cell, AAV, blood–retinal barrier, inner limiting membrane

## Introduction

Müller cells are the principal glial cell of the retina. They provide architectural support stretching radially across the thickness of the neural layers and their endfeet form the limits of the retina at the outer and inner limiting membranes, respectively. Additionally, Müller cells are intimately connected with retinal endothelial cells, pericytes, and astrocytes to establish the blood–retinal barrier (BRB) limiting material transport between the bloodstream and the retina (Hosoya and Tachikawa, 2012). Conditional Müller cell ablation leads to rapid and intense focal vascular leakage (Shen et al., 2012) showing the crucial role of these cells in the maintenance of this barrier. In the clinic, BRB breakdown is seen in retinal detachment, inflammatory eye diseases, age-related macular degeneration (AMD), and in macular

oedema, an important complication of numerous injuries and ocular diseases such as uveitis, diabetic retinopathy (DR), and macular telangiectasia (MacTel 2). In MacTel 2 and in DR, Müller cell loss and abnormalities have been observed associated with BRB breakdown. Currently, there is no good transgenic animal model to study diseases with BRB breakdown because these pathologies are not purely genetic but multifactorial. In previous work, we have shown that the absence of Dystrophin Dp71 in Müller cells causes a breakdown of the BRB emulating some hallmarks associated with these diseases.

Dp71 is a membrane-bound cytoskeletal protein localized at the Müller cell endfeet participating in ion and water homeostasis (Tadayoni et al., 2012). The Dp71 knockout mouse (Sarig et al., 1999) shows a blood–retinal barrier (BRB) permeability together with a redistribution of the ion channels

View this article online at [wileyonlinelibrary.com](http://wileyonlinelibrary.com). DOI: 10.1002/glia.22617

Published online Month 00, 2013 in Wiley Online Library ([wileyonlinelibrary.com](http://wileyonlinelibrary.com)). Received June 12, 2013, Accepted for publication Nov 22, 2013.

Address correspondence to: Alvaro Rendon, Institut de la Vision/INSERM/UPMC, Univ Paris 06/CNRS/CHNO des Quinze-Vingts, Paris, France. E-mail: [alvaro.rendon@inserm.fr](mailto:alvaro.rendon@inserm.fr) and Deniz Dalkara, Institut de la Vision/INSERM/UPMC, Univ Paris 06/CNRS/CHNO des Quinze-Vingts, Paris, France. E-mail: [deniz.dalkara@inserm.fr](mailto:deniz.dalkara@inserm.fr)

From the <sup>1</sup>Institut de la Vision/INSERM/UPMC, Univ Paris 06/CNRS/CHNO des Quinze-Vingts, Paris, France; <sup>2</sup>University of California Berkeley, Department of Bioengineering, Department of Chemical Engineering, Helen Wills Neuroscience Institute; <sup>3</sup>University of California Berkeley, Department of Molecular and Cell Biology, Helen Wills Neuroscience Institute; <sup>4</sup>Fondation Ophthalmologique Adolphe de Rothschild, Paris, France; <sup>5</sup>Institute of Ophthalmology, University College of London, United Kingdom; <sup>6</sup>Académie des Sciences–Institut de France, Paris, France.

Additional Supporting Information may be found in the online version of this article.

Kir4.1, the water transport protein, Aquaporin 4 (AQP4), and the  $\beta$ -dystroglycan throughout the Müller cells, as well as a down-regulation of the AQP4 and  $\beta$ -dystroglycan (Fort et al., 2008). Dramatic morphological modification of the Müller cell endfeet occurs in the absence of Dp71. Müller cell endfeet become slack and spread due to the lack of anchoring through Dp71 (Fort et al., 2008) and vascular permeability increases (Sene et al., 2009). Similarly, in retinal detachment, Dp71 protein becomes down-regulated, leading to increased retinal vascular permeability (Sene et al., 2009). These findings collectively suggest that Dp71-null mouse can be used as an animal model with permeable BRB emulating a number of hallmarks of retinal detachment, diabetic retinopathy or age-related macular degeneration (patents No. 08 305381.9, 2008; and No. EP09305608.3, 2010). As Müller cells are involved in virtually all the pathological processes concerning the retina, we wanted to investigate their participation in the BRB permeability that occurs in the Dp71-null mice at a morphological level. To this aim, we fluorescently labeled Müller cells of the Dp71-null mouse, using an Adeno-associated virus (AAV) variant, ShH10-GFP, engineered to target Müller cells specifically (Klimczak et al., 2009). In the Dp71-null mouse, we noted that the Müller cells are transduced throughout the retina, whereas Müller cell transduction follows the large retinal blood vessels at the inner surface of the retina in the normal mouse retinas. The endfeet of the Dp71 deficient Müller cells do not wrap around the vasculature as they do in the wild-type retinas. Furthermore, we found that these cells are transduced more intensely in absence of Dp71, insinuating a better viral access to the retina in this mouse model.

A long-term perspective of this work is to develop AAV-based gene therapies for diseases with permeable BRB. These gene therapies need to account for a retina with compromised barriers. Information on how AAV vectors behave in retinas displaying some hallmark symptoms of diseases with increased vascular permeability is timely. We have thus examined the increased retinal transduction observed using AAV in more detail in the Dp71-null model. As Müller cell endfeet are considered part of the inner limiting membrane, we inquired if this barrier might also be compromised in addition to the BRB, in this mouse. Previous work has shown that AAV injected into the vitreous both binds and accumulates at the ILM (AAV2, AAV8, and AAV 9) or diffuses away from the retina if binding sites are unavailable (AAV1 and AAV5) (Dalkara et al., 2009). Changes in the transduction patterns are most obvious with AAV5 vectors administered intravitreally, as this vector incapable of infecting the wild-type retina leads to the most robust pattern of gene expression when the inner limiting membrane is breached. Indeed, intravitreal delivery of AAV5 led to intense and selective labeling of photoreceptor cells in the Dp71-null retina indicating the ILM

becomes permeable to AAV in absence of Dp71. This finding indicates that invasive subretinal injections can be avoided as even the outer retina can be reached through intravitreal AAV administration in the absence of Dp71.

Another consideration in the development of gene therapies in diseases with compromised BRB is virus leakage into the bloodstream. The successful application of AAV in ocular gene therapy in the clinic (Bainbridge et al., 2008; Cideciyan et al., 2008; Maguire et al., 2008) is largely due to the lack of spread of virus from the injection site, which minimizes systemic dissemination of the virus and the possibility of unwanted systemic side effects following intraocular delivery. Here we demonstrate that, in the Dp71-null mice, the ILM is highly permeable to different AAV serotypes after an intravitreal injection whereas the BRB remains impermeable to AAV particles, an important consideration for the safety of gene therapies for diseases with compromised BRB.

## Materials and Methods

### Animals

The Dp71-null mice (Sarig et al., 1999) was a kind gift from Pr David Yaffe and were produced by replacing, via homologous recombination, most of the first and unique exon of Dp71 and of a small part of Dp71 first intron with a sequence encoding a  $\beta$ -gal-neomycin-resistance chimeric protein ( $\beta$ -geo). In this mouse line, Dp71 expression is abolished without interfering with the expression of other products of the DMD (Duchenne Muscular Dystrophy) gene. C57BL/6J mice strain (JANVIER, France) was used as controls for this study. All animals used in this study were cared for and handled according to the ARVO Statement for the Use of Animals in Ophthalmic and Vision Research.

### Generation and Purification of AAV Vectors

Recombinant AAVs were produced by the plasmid co-transfection method (Choi et al., 2007a, 2007b), and the resulting lysates were purified via iodixanol gradient ultracentrifugation as previously described. Briefly 40% iodixanol fraction was concentrated and buffer exchanged using Amicon Ultra-15 Centrifugal Filter Units. Vector stocks were then tittered for DNase-resistant vector genomes by real-time PCR relative to a standard (Aurnhammer et al., 2012).

### Injections

Before vector administration, mice were anesthetized with ketamine (50 mg/kg) and xylazine (10 mg/kg Rompum). Pupils were dilated by the ocular instillation of neosynephrine 5% Faure (Europhtha) and mydriaticum 0.5% (Théa) eye drops. An ultrafine 30-gauge disposable needle was passed through the sclera, at the equator and next to the limbus, into the vitreous cavity. Injection of 1  $\mu$ L stock containing  $1-4 \times 10^{11}$  vp, was made with direct observation of the needle in the center of the vitreous cavity. Left eyes were injected and right eyes were served as control.

### Fundus Photography

Fundus examinations were performed at 7, 14, 21 and 28 days after the intravitreal injection of AAV5 or ShH10 coding GFP under the

ubiquitous CAG promoter. Fundus photographs were obtained with a scanning laser ophthalmoscope (SLO) (HRA, Heidelberg, Germany) or a Micron III fundus camera. Mouse pupils were dilated by the application of neosynephrine (5%) and mydriaticum (0.5%) eye drops prior to imaging.

### Optical Coherence Tomography

Optical Coherence Tomography (OCT) was performed using an SD-OCT system (Biotigen Inc., Durham, NC). Hydration with normal saline was used to preserve corneal clarity. Volume analysis centered on the optic nerve head was performed, using 100 horizontal, raster, and consecutive B-scan lines, each one composed of 1200 A-scans. The volume size was  $1.4 \times 0.1$  mm on either side of the optic nerve. A custom software was used to generate the en face fundus image using reflectance information obtained from the OCT sections (volume intensity projection), so that the point-to-point correlation between OCT and fundus position was possible and accurate.

### PCR Analysis of Mouse Blood Samples

Genomic DNA from blood samples was extracted using QIAamp® DNA Micro Kit (QIAGEN, Germany) according to the manufacturer's instructions. PCR amplifications of genomic DNA were performed using GoTaq® DNA polymerase (Promega, USA) on a ThermoCycler instrument (Applied Biosystem). PCR primers were designed using Primer3 software. The following primer pair was used: GFP, sense 5'-CGACACAATCTGCCCTTTCG-3', antisense 5'-CATGGACGAGCTGTACAAGGGA-3'.

### Immunocytochemistry

One month after vector injection, enucleated eyes were dissected to remove lens and cornea, and fixed by immersion in 4% paraformaldehyde for 1 h. Fixed eyes were cryoprotected in 30% sucrose, frozen and embedded in Cryomatrix (Thermo Shandon). Cryosections of 10  $\mu$ m were cut and mounted on SuperFrost/Plus slides (Microm). Sections were permeabilized for 10 min with 0.1% Triton X100 in PBS (Phosphate Buffer Saline) and blocked for 1 h with 1% bovine serum albumin, 0.1% Tween 20 in PBS. For retinal flatmounts, enucleated eyes were immersion fixed in 4% paraformaldehyde for 10 min. Retinas were separated from the RPE and sclera by cutting around the ora serrata and cutting the optic nerve. For agarose sections, fixed retinas were rinsed in PBS, embedded in warm 5% agarose (type XI, Sigma) and sectioned at 100  $\mu$ m with a vibratome (Leica, Allendale, NJ). Tissues were then incubated with primary antibodies in blocking buffer at 4°C overnight. The antibodies used are as follows: anti-GFAP antibody (Z0334, Dako) 1/1500, anti-laminin (L9393, Sigma) 1/1000, anti-rhodopsin clone 4D2 (MABN15, Millipore) 1/500, anti-glutamine synthetase clone GS-6 (MAB302, Millipore) 1/1500, PNA Lectin (L32459, Invitrogen) 1/40; Lectin from *Bandeiraea simplicifolia* TRITC conjugate (L5264, Sigma) 1/80. After several washes with PBS, secondary antibodies (Interchim, France) coupled to Alexa fluor (Invitrogen, France) were used diluted 1:800 for 1 h at room temperature. Retinas were mounted with Fluorsave reagent (Calbiochem). Confocal microscopy was performed on an Olympus FV1000 laser-scanning confocal

microscope. Images were acquired sequentially, line by line, in order to reduce excitation and emission crosstalk, step size was defined according to the Nyquist–Shannon sampling theorem. Exposure settings that minimized oversaturated pixels in the final images were used. Twelve bit images were then processed with FIJI, Z-sections were projected on a single plane using maximum intensity under Z-project function and finally converted to 8-bit RGB color mode.

### Data Analysis

Results are expressed as mean  $\pm$  standard error of the mean (SEM). Confocal stacks of 50 images were taken with the same settings. These images were Z projected and the fluorescence area was quantified with Fiji (Fiji Is Just ImageJ) software. Fluorescence data were then analyzed using Mann–Whitney *U* test with Prism 5 (GraphPad Software, San Diego, CA). *P* values <0.05 accepted as statistically significant.

## Results

### ShH10-GFP Targets Müller Glial cells in the Wild-type Mouse Retina

Previously, the AAV variant ShH10, engineered for specific glial transduction by directed evolution, has been characterized in rat retinas (Klimczak et al., 2009) and has been shown to transduce almost exclusively the Müller cells with small amount of off target expression in RGCs. To validate the Müller cell specificity of this virus in mouse retina, we injected intravitreally  $1-4 \times 10^{11}$  vg of ShH10 coding GFP under the control of a ubiquitous promoter. Injections were done in 7-week-old mice and followed weekly by *in vivo* fluorescence imaging up to 4 weeks after injection ( $n = 10$ ). We observed that GFP expression peaked at day 7 and remained constant thereafter (Fig. 1A). Histological examination of GFP expression in retinal flatmounts revealed a strong expression pattern localized near major vasculature and the optic nerve (Fig. 1B). Confocal imaging of retinal cross-sections (Fig. 1C) and retinal flatmounts (Fig. 1) after GFAP immunostaining, showed exclusive Müller cell transduction using ShH10 and no GFP expression in astrocytes or retinal ganglion cells (RGCs). In conclusion, in wild-type mice ShH10-GFP is highly selective for Müller cells.

### Müller Cell Transduction with ShH10-GFP in the Dp71-null Mouse Retina

To assess Müller cell morphology in the Dp71-null mice, ShH10-GFP was delivered at an equal titer into the vitreous of Dp71-null mice ( $n = 10$ ). Transduction patterns were compared to wild-type retinas, by scanning laser ophthalmoscope (SLO) (Fig. 2A and B) 15 days post-injection. One month post-injection in flatmounted retinas (Fig. 2C and D) were imaged and contrasted. Figure 2C and D shows representative images of GFP fluorescence in the two mouse models. Dp71-null mice show a more widespread and higher intensity Müller cell transduction compared to wild-type mice ( $n = 6$ ).

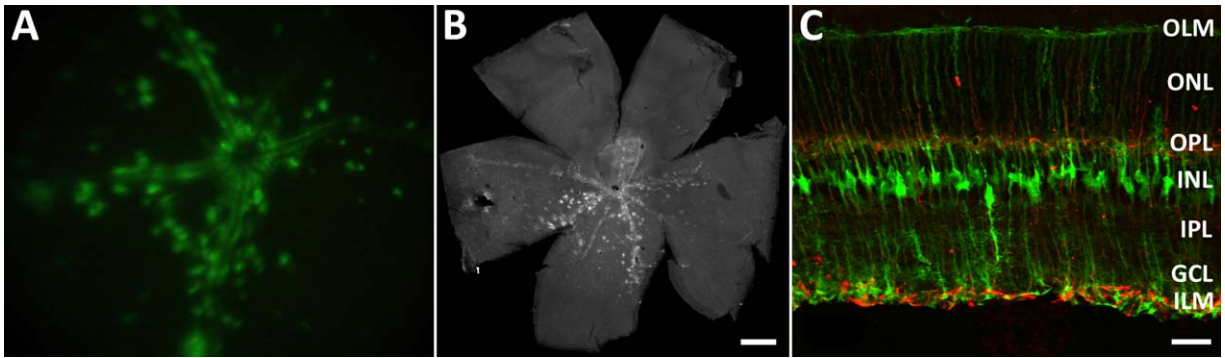


**FIGURE 1:** ShH10 transduces Müller cells around retinal vasculature in the wild-type retina. Four weeks after ShH10-GFP injection: (A) Fundus image of an adult mouse showing GFP expression around retinal blood vessels, (B) flatmounted retina of the left eye intravitreally injected with ShH10 showing the same GFP expression pattern (scale bar: 500  $\mu\text{m}$ ), and (C) confocal image of a retinal cryosection shows exclusive Müller cell transduction (scale bar: 20  $\mu\text{m}$ ).

The numbered rectangles on flatmounted retinas (Fig. 2C and D) represent the four representative areas used for confocal images in Fig. 2E and F. Using these confocal stacks acquired using the same settings, we compared the transduction levels in the Müller cells by quantifying the extent of GFP labeled area and GFP intensity for each retina (Fig. 2G and H). The fluorescence area was approximately twofold larger in the Dp71-null than in the wild-type mice and the fluorescence intensity was approximately sixfold higher in the Dp71-null than in the wild-type mice. Interactions between GFP labeled Müller glia and astrocytes were examined using higher magnification confocal images following GFAP labeling. This showed that ShH10 did not transduce any astrocytes (Fig. 2I and J) and similar interactions were observed between astrocytes and blood vessels in both the retinas. We also confirmed the high selectivity of ShH10 for Müller cells on agarose sections in Dp71-null mice showing there is no expression in other cell-types using ShH10 (Supporting Information, Fig. S1). These results collectively show that the Müller cells can be more easily and intensively transduced by ShH10 in absence of Dp71. Furthermore, labeling of the Müller cells shows their endfeet are more spread-out in absence of Dp71 than those of wild-type mice, confirming previous observations (Fort et al., 2008).

### **The Inner Limiting Membrane is Altered in the Dp71-null Mice**

The Müller cell endfeet are deformed in absence of Dp71 (Fort et al., 2008), and this leads to changes in the structure of the inner limiting membrane (ILM) in addition to the previously described leakiness of the BRB. To compare the characteristics of the ILM in wild-type and Dp71-null mice, cross-sections of Dp71-null retinas with GFP labeled Müller cells were examined in relation to the ILM. The ILM was labeled with an anti-laminin antibody as laminin is a major component of the ILM secreted by Müller cell endfeet (Half-

ter et al., 2008). Our data shows that the ILM is thinner and compacted around the Müller cell endfeet in retinal cross-sections (Fig. 3A–D). This provides evidence for thinning of the ILM in the Dp71-null retinas through the delocalization of laminin in absence anchoring through  $\beta$ -dystroglycan.

Prior studies have shown that Kir4.1 and AQP4 associate with the Dp71-dependent DAPs complex at the Müller cell endfeet and that this complex associates with laminin through  $\beta$ -dystroglycan (Hirrlinger et al., 2011) (Fig. 3G). It is known that Dp71 absence is correlated with a profound reorganization in Müller cells including the compensatory up-regulation and redistribution of utrophin along the Müller cell body, a dramatic decrease of AQP4 expression, a significant decreased expression and redistribution of  $\beta$ -dystroglycan along with the increased expression and redistribution of  $\alpha$ -dystrobrevin and the redistribution of Kir4.1. These important intracellular perturbations are reflected by a lack of interaction of the DAPs complex with ILM components outside the Müller cell.

In wt retinas, laminin forms a homogenous layer at the Müller cell endfeet covering the vitreo-retinal junction. In contrast, Dp71-null retinas show heterogeneous distribution of laminin, with intensely labeled and unevenly distributed patches of laminin across the retina (Fig. 3E, F).

In addition to the observations about ILM thickness, we observed that all layers of Dp71-null mouse retinas were thinner than those of the wild-type mice (Supporting Information, Fig. S2). Retinal thickness loss as well as the ECM becoming more porous in the absence of Dp71 can be additional factors contributing to the improvement in AAV transduction. *In vivo* OCT imaging confirmed our histological observations of retinal thickness. OCT imaging was performed at 100  $\mu\text{m}$  around the optic nerve on 8 eyes of each strain. Following measurements were made after Z projection of OCT images at 500  $\mu\text{m}$  from the optic nerve (Supporting Information, Fig. S2A): (i) the whole retina, from the retinal

pigment epithelium (RPE) to the ganglion cell layer (GCL); (ii) the photoreceptor layer composed of the outer segments (OS) and the inner segments (IS); (iii) the outer nuclear layer

(ONL); (iv) and the inner retina consisting of the inner nuclear layer (INL), the inner plexiform layer (IPL), the GCL, and the ILM (Supporting Information, Fig. S2B). After statistical analysis, we showed that each retinal cell layer is significantly thinner in Dp71-null mice than in wild-type mice (Supporting Information, Fig. S2C).

**Intravitreal Injection of AAV5-GFP Strongly Transduces Photoreceptors in Dp71-null Mouse Retina**

It has been shown that the mild digestion of the ILM with a non-specific protease enhanced transduction of multiple retinal cell types from the vitreous, with AAV5 mediating particularly remarkable expression at the photoreceptor layer (Dalkara et al., 2009). AAV5 is known to only transduce the photoreceptor cells when it is injected subretinally or when the ILM of the retina is disrupted (Dalkara et al., 2009; Kolstad et al., 2010; Li et al., 2009). Based on this knowledge, we tested the ability of AAV5 to transduce retinal photoreceptors after injection into the vitreous of Dp71-null mice testing the hypothesis of a disrupted ILM. As anticipated, one month after intravitreal injection of AAV5-GFP ( $n = 6$ ), we obtained strong photoreceptor transduction across the entire retina in the Dp71-null mice (Fig. 4B and C) whereas in the wild-type retina there was no detectable GFP expression (Fig. 4A). Agarose sections further confirm GFP expression restricted to the photoreceptor layer (Fig. 4D–F). The overall reduction in thickness of the retina might also contribute to this phenomenon observation.

**The Blood–retinal Barrier of the Dp71-null Mice is not Permeable to AAVs**

Knowing that in the Dp71-null mouse, the BRB is leaky to certain molecules as large as BSA, we wanted to test the extent of this permeability for particles, such as AAV. We checked if intravitreally injected ShH10-GFP can cross the BRB to go into the bloodstream. We collected blood from

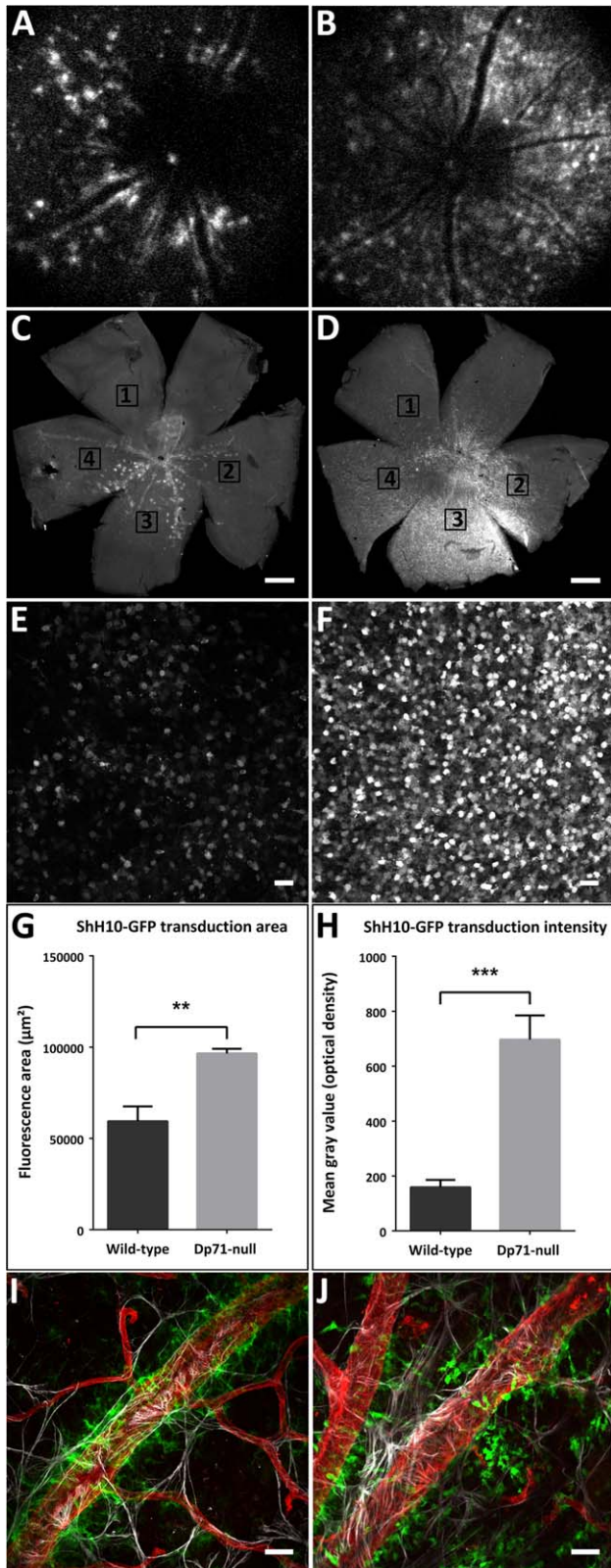


**FIGURE 2:** Müller cells are transduced more widely and strongly in the Dp71-null retina. SLO images two weeks post ShH10-GFP injection in wild type (A) and Dp71-null (B) retinas *in vivo*. *Ex vivo* imaging of flatmounted retinas (scale bar: 500  $\mu\text{m}$ ) of wild-type (C) and Dp71-null (D) mouse retinas one month after ShH10-GFP ( $4 \times 10^{11}$  vp) injection. Confocal stacks in (C) and (D) were used to quantify GFP expression levels around the Müller cell nuclei (scale bar: 20  $\mu\text{m}$ ). (G) The GFP fluorescent area ( $P = 0.0011$ , Mann–Whitney  $U$  test). (H) The GFP intensity ( $P = 0.0002$ , Mann–Whitney  $U$  test) in wild-type and Dp71-null mice ( $n = 16$ ). Higher magnification confocal images of ShH10 treated retinal flatmounts using lectin from *Bandeiraea simplicifolia* (red), anti-GFAP (grey) and DAPI (blue) (I) wild-type retina and (J) Dp71-null retina. Labeling of the Müller cells (green) shows endfeet more spread-out in absence of Dp71 than those of wild-type mice (scale bar: 20  $\mu\text{m}$ ).

wild-type and Dp71-null mice 24, 48 and 72 h after intravitreal injection of ShH10-GFP and measured the presence of viral DNA in the collected blood for each time point using PCR. We were not able to amplify GFP DNA from the bloodstream of either mouse strain indicating that the BRB is not permeable to virus when they are injected into the vitreous (Supporting Information, Fig. S4, lanes 4–5, 8–9,

12–13). As a positive control, AAV injected into the bloodstream through the penile vein clearly showed presence of the GFP transgene in the circulation (data not shown). This result is reassuring for the development of ocular gene therapy aimed at treating diseases showing a BRB breakdown.

### Discussion

Several retinal diseases are associated with a blood–retinal barrier breakdown phenotype and understanding the molecular mechanisms that contribute to the integrity of retinal barriers is of importance. The Dp71-null mouse is a good animal model to study the involvement of Müller glia in maintaining retinal barriers. Indeed, the absence of Dp71, most abundantly expressed in Müller glial cells, leads to the blood–retinal barrier breakdown in this mouse.

In order to understand the involvement of Müller glia in retinal permeability in the Dp71-null mouse, we used an engineered AAV variant called ShH10 to label these cells. We then compared the interaction among Müller glia, retinal vasculature (BRB), and inner limiting membrane in the Dp71-null retina in comparison to a wild-type retina. ShH10 led to specific and efficient transgene expression in Müller glia, both in the Dp71-null and wild-type retinas (Fig. 5, arrow 1). However, the transduction patterns were found to be strikingly different in these two retinas. In the wild-type mouse, ShH10 led to intense and specific transduction of Müller cells in proximity to retinal blood vessels. It is well known that the ILM is thinner at the site of the major retinal blood vessels (Yanoff and Fine, 1996), and the Müller glial endfeet wrap around the blood vessels which explain this typical transduction pattern alongside the major vasculature observed after intravitreal injection of AAV particles in a normal retina. Interestingly, in the Dp71-null mouse, ShH10 transduced a larger area of the retina, and led to stronger gene expression in the Müller cells. This reflects better viral access to Müller cell endfeet in the Dp71-null mouse. In absence of Dp71, the Müller cell endfeet are larger and more spread-out (Fort et al., 2008) presenting a larger contact surface for the virus

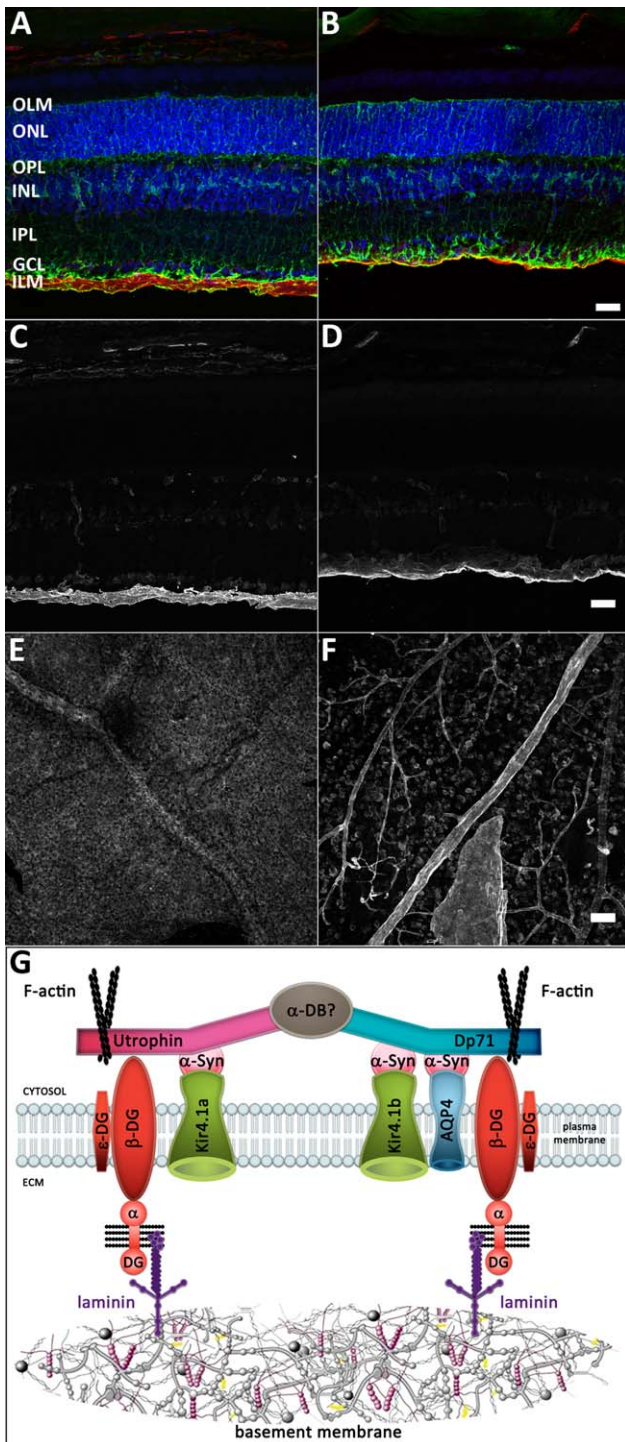


**FIGURE 3:** Comparative analysis of the ILM thickness in Dp71-null and wild-type retinas. Cryosection of a wild-type (A) and a Dp71-null (B, scale bar: 25  $\mu$ m) mice retina labeled with DAPI (blue) to visualize the nuclei, anti-glutamine synthetase antibody (green) for the Müller cells and pan-laminin antibody to show the inner limiting membrane (scale bar: 25  $\mu$ m). (C–D) Labeling in images (A) and (B) with a pan-laminin antibody (grey), prior to merging the colors of different channels. Flatmount images of a wild-type (E) and a Dp71-null (F) retina, after laminin labeling (scale bar: 50  $\mu$ m). (G) Hypothetical model of Dp71- and Utrophin-DAPs complexes binding laminins in the ILM showing the close link between Dp71, dystroglycans, and laminins and illustrating how the absence Dp71 can affect laminins and significantly alters organization of the ILM.

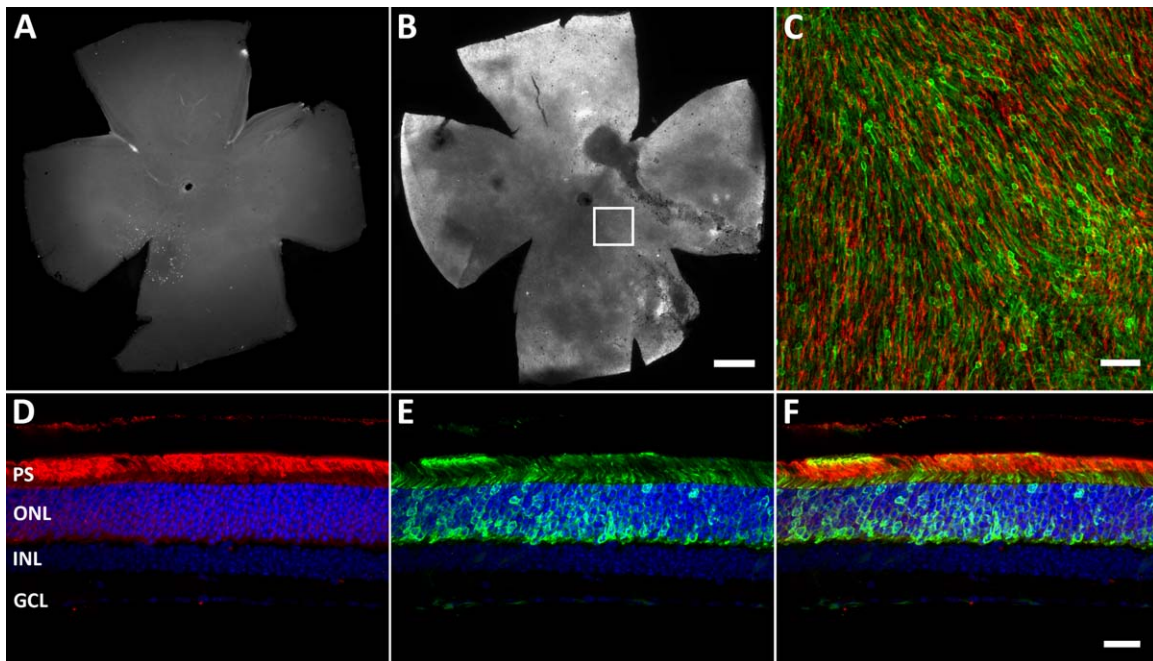


**FIGURE 4: Efficient photoreceptor transduction with AAV5-GFP in Dp71-null mouse retina. (A)** Flatmount of a wild-type retina imaged at 28 days after intravitreal injection of AAV5. **(B)** Flatmount of a Dp71-null mouse retina showing strong fluorescence on the photoreceptor side 4 weeks after intravitreal injection of AAV5 (scale bars: 500  $\mu\text{m}$ ). **(C)** Higher magnification image of the area indicated by the white rectangle in panel B (scale bar: 30  $\mu\text{m}$ ). **(D-F)** Agarose sections of the Dp71-null mice retina transduced by the AAV5-GFP showing **(D)** rods labeled by rho4d2, **(E)** the photoreceptors expressing GFP and **(F)** the merged of D and E to colocalize the GFP expression and the rods (scale bars: 20  $\mu\text{m}$ ).

at the ILM. Retinal basement membranes serve as attachment sites for Müller cells on the ILM, providing polarity cues to adherent cells. Laminin is a key component of ILM throughout development, suggesting that it plays key roles in its organization. Our study shows that the absence of Dp71 affects laminins and significantly alters organization of the inner limiting membrane. Mice with compound deletion of both the  $\beta 2$  and the  $\gamma 3$  laminin genes show similar disruption of the ILM (Pinzon-Duarte et al., 2010) supporting our observations. Laminins bind to a variety of cell-surface receptors, including integrins, dystroglycan, sulfated glycolipids, and syndecans (Durbecq, 2010) (Fig. 3G). Therefore, it is not surprising that in the absence of dystroglycan, laminins become disorganized both at the ILM and within the ECM. This visible disorganization of the ILM substantiated by laminin is the mechanistic basis for the increased permeability of the Dp71-null retina to AAV particles. All of these phenomena involving Müller cells and Dp71 likely contribute to the overall thinning of the retina in absence of Dp71 as well as to the thinning and permeabilization of the retinal barriers.

The thinning of the ILM is particularly important from a viral transduction standpoint as intravitreal administration of AAV vectors are hindered by the presence of this membrane (Dalkara et al., 2009; Ivanova et al., 2010; Yin et al., 2011). Intravitreal administration route is a preferred administration route to access the retina as it is non-invasive and

leads to pan-retinal delivery. Current gene delivery methods require an injurious subretinal injection to reach the outer retina and only transduce a fraction of the retina (Jacobson et al., 2012). There have been several studies shedding light onto how ILM acts as a barrier to retinal transduction by AAVs (Aartsen et al., 2010; Cehajic-Kapetanovic et al., 2011; Dalkara et al., 2009; Kolstad et al., 2010). Previously it has been shown that mild digestion of the ILM with a non-specific protease, increases viral access to the retina (Dalkara et al., 2009). Similarly, it has been demonstrated (Aartsen et al., 2010) that Müller glial cell transduction by AAV6, an AAV serotype similar to ShH10, is improved by a disruption of the ILM by collagenase treatment. In this latter study, the pattern of GFP expression follows the major vessels in the wild-type retina whereas GFP expression increases throughout the retina after mild digestion of the ILM with collagenase, similar to our observations in the Dp71-null retina. In parallel, it has been shown that retinal degenerative disease can cause the ILM to become compromised providing better access to viral particles (Kolstad et al., 2010). Altogether, these findings led us to hypothesize that the absence of Dp71 might lead to a more permissive ILM. Since the selective visualization of the ILM is challenging, we tested the hypothesis of a leaky ILM by applying another AAV serotype, which cannot transduce retinal cells across an intact ILM. AAV serotype 5 is able to transduce the retinal photoreceptors when

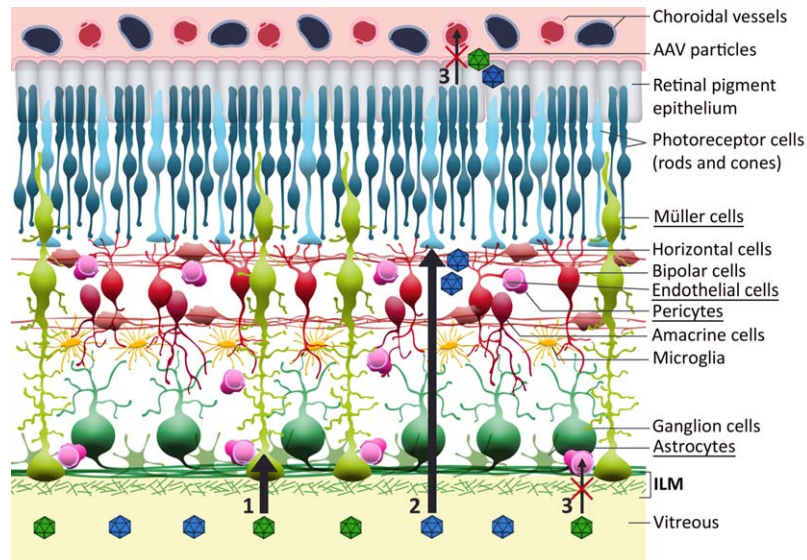


**FIGURE 5:** Schematic representation of a Dp71-null mouse retina after intravitreal injection of AAV. The arrow 1 represents the enhanced transduction of Müller cells by ShH10 in the Dp71-null mouse. The arrow 2 shows the efficient transduction of photoreceptors by AAV5 because of the altered ILM of the Dp71-null mouse. The arrow 3 highlights that the BRB breakdown of the Dp71-null mouse retina does not allow the passage of viruses into the bloodstream.

applied subretinally yet it does not lead to retinal transduction when applied into the vitreous of wild-type rodents as its primary attachment receptors are shielded by the ILM and inner neurons. We observed that AAV5 leads to pan-retinal photoreceptor transduction in the Dp71-null mouse confirming that the ILM of this mouse strain is permissive (Fig. 5, arrow 2) allowing deeper retinal access to this serotype. As a perspective, we can imagine that transient inhibition of Dp71 via siRNA might be a promising way to increase photoreceptor transduction allowing AAVs such as AAV5 to be delivered through the vitreous.

Dp71 expression is down-regulated after retinal detachment, proving the key role of this protein in the maintenance of a normal BRB permeability. Thus, Dp71 expression can potentially restore the barrier properties of the Müller cell endfeet if we can provide the protein exogenously. In this context, this preliminary study of AAV-mediated targeting of Müller glia sets the basis for developing retinal gene therapy aimed at restoring Dp71 expression in retinal disease with leaky BRB. A potential obstacle for the development of AAV gene therapy for eye diseases with compromised BRB is the leakage of virus into the bloodstream. We thus analyzed blood samples from mice intravitreally injected with ShH10-GFP to detect the presence of viral particles in the bloodstream. We found no evidence of the GFP transgene in the circulation of Dp71-null or wild-type mice after intravitreal administration of ShH10 (Fig. 5, crossed arrow 3).

In conclusion, the ILM of Dp71-null mouse is thinner and more permeable to several AAV serotypes after intravitreal injection while the BRB of these mice remains selective

for AAV particles. These findings are reassuring for the development of gene therapies for diseases with compromised BRB and the Dp71-null mouse offers a good model for the study of pathologies showing a BRB breakdown such as AMD, diabetic retinopathy, and the MacTel 2.

### Acknowledgment

Grant sponsor: Association Française contre les Myopathies (AFM); Grant number: 14853 (to A.R.).

We acknowledge the Association Française contre les Myopathies (AFM) for a PhD fellowship to O.V. and Allergan INC. This work performed in the frame of the LABEX LIFESENSES [reference ANR-10-LABX-65] was supported by French state funds managed by the ANR. We thank Meike Visel, Peggy Barbe, and Mélissa Desrosiers for technical assistance with AAV preparations and Romain Bénard for assistance in retinal injections. We also sincerely thank Adeline Berger and Sophie Cavallero for their excellent expertise in OCT imaging. We are grateful to Stéphane Fouquet for excellent technical assistance in confocal microscopy and his expert input with the interpretation of the results. We earnestly thank Sékou Fofana for his valuable help for the graphic design of our schemes. We also acknowledge Michel Paques for skillful assistance in SLO imaging. Finally, we are very grateful to Ramin Tadayoni for his support and accurate analysis of our results.

### References

Aartsen WM, van Cleef KW, Pellissier LP, Hoek RM, Vos RM, Blits B, Ehlert EM, Balaggan KS, Ali RR, Verhaagen J, Wijnholds J. 2010. GFAP-driven GFP

- expression in activated mouse Muller glial cells aligning retinal blood vessels following intravitreal injection of AAV2/6 vectors. *PLoS One* 5(8):e12387.
- Aurnhammer C, Haase M, Muether N, Hausl M, Rauschhuber C, Huber I, Nitschko H, Busch U, Sing A, Ehrhardt A, Baiker A. 2012. Universal real-time PCR for the detection and quantification of adeno-associated virus serotype 2-derived inverted terminal repeat sequences. *Hum Gene Ther Methods* 23(1):18–28.
- Bainbridge JW, Smith AJ, Barker SS, Robbie S, Henderson R, Balaggan K, Viswanathan A, Holder GE, Stockman A, Tyler N, Petersen-Jones S, Bhattacharya SS, Thrasher AJ, Fitzke FW, Carter BJ, Rubin GS, Moore AT, Ali RR. 2008. Effect of gene therapy on visual function in Leber's congenital amaurosis. *N Engl J Med* 358(21):2231–2239.
- Cehajic-Kapetanovic J, Le Goff MM, Allen A, Lucas RJ, Bishop PN. 2011. Glycosidic enzymes enhance retinal transduction following intravitreal delivery of AAV2. *Mol Vis* 17:1771–1783.
- Choi VW, Asokan A, Haberman RA, Samulski RJ. 2007a. Production of recombinant adeno-associated viral vectors. *Curr Protoc Hum Genet Chapter 12:Unit 12 9*.
- Choi VW, Asokan A, Haberman RA, Samulski RJ. 2007b. Production of recombinant adeno-associated viral vectors for in vitro and in vivo use. *Curr Protoc Mol Biol Chapter 16:Unit 16 25*.
- Cideciyan AV, Aleman TS, Boye SL, Schwartz SB, Kaushal S, Roman AJ, Pang JJ, Sumaroka A, Windsor EA, Wilson JM, Flotte TR, Fishman GA, Heon E, Stone EM, Byrne BJ, Jacobson SG, Hauswirth WW. 2008. Human gene therapy for RPE65 isomerase deficiency activates the retinoid cycle of vision but with slow rod kinetics. *Proc Natl Acad Sci U S A* 105(39):15112–15117.
- Dalkara D, Kolstad KD, Caporale N, Visel M, Klimczak RR, Schaffer DV, Flannery JG. 2009. Inner limiting membrane barriers to AAV-mediated retinal transduction from the vitreous. *Mol Ther* 17(12):2096–2102.
- Durbeej M. 2010. Laminins. *Cell Tissue Res* 339(1):259–268.
- Fort PE, Sene A, Pannicke T, Roux MJ, Forster V, Mornet D, Nudel U, Yaffe D, Reichenbach A, Sahel JA, Rendon A. 2008. Kir4.1 and AQP4 associate with Dp71- and utrophin-DAPs complexes in specific and defined microdomains of Muller retinal glial cell membrane. *Glia* 56(6):597–610.
- Halfter W, Dong S, Dong A, Eller AW, Nischt R. 2008. Origin and turnover of ECM proteins from the inner limiting membrane and vitreous body. *Eye (Lond)* 22(10):1207–1213.
- Hirrlinger PG, Pannicke T, Winkler U, Claudépierre T, Varshney S, Schulze C, Reichenbach A, Brunken WJ, Hirrlinger J. 2011. Genetic deletion of laminin isoforms beta2 and gamma3 induces a reduction in Kir4.1 and aquaporin-4 expression and function in the retina. *PLoS One* 6(1):e16106.
- Hosoya K, Tachikawa M. 2012. The inner blood-retinal barrier: molecular structure and transport biology. *Adv Exp Med Biol* 763:85–104.
- Ivanova E, Hwang GS, Pan ZH, Troilo D. 2010. Evaluation of AAV-mediated expression of Chop2-GFP in the marmoset retina. *Invest Ophthalmol Vis Sci* 51(10):5288–5296.
- Jacobson SG, Cideciyan AV, Ratnakaram R, Heon E, Schwartz SB, Roman AJ, Peden MC, Aleman TS, Boye SL, Sumaroka A, Conlon TJ, Calcedo R, Pang JJ, Erger KE, Olivares MB, Mullins CL, Swider M, Kaushal S, Feuer WJ, Iannaccone A, Fishman GA, Stone EM, Byrne BJ, Hauswirth WW. 2012. Gene therapy for leber congenital amaurosis caused by RPE65 mutations: safety and efficacy in 15 children and adults followed up to 3 years. *Arch Ophthalmol* 130(1):9–24.
- Klimczak RR, Koerber JT, Dalkara D, Flannery JG, Schaffer DV. 2009. A novel adeno-associated viral variant for efficient and selective intravitreal transduction of rat Muller cells. *PLoS One* 4(10):e7467.
- Kolstad KD, Dalkara D, Guerin K, Visel M, Hoffmann N, Schaffer DV, Flannery JG. 2010. Changes in adeno-associated virus-mediated gene delivery in retinal degeneration. *Hum Gene Ther* 21(5):571–8.
- Li W, Kong F, Li X, Dai X, Liu X, Zheng Q, Wu R, Zhou X, Lu F, Chang B, Li Q, Hauswirth WW, Qu J, Pang JJ. 2009. Gene therapy following subretinal AAV5 vector delivery is not affected by a previous intravitreal AAV5 vector administration in the partner eye. *Mol Vis* 15:267–275.
- Maguire AM, Simonelli F, Pierce EA, Pugh EN, Jr., Mingozzi F, Bennicelli J, Banfi S, Marshall KA, Testa F, Surace EM, Rossi S, Lyubarsky A, Arruda VR, Konkle B, Stone E, Sun J, Jacobs J, Dell'Osso L, Hertle R, Ma JX, Redmond TM, Zhu X, Hauck B, Zelenia O, Shindler KS, Maguire MG, Wright JF, Volpe NJ, McDonnell JW, Auricchio A, High KA, Bennett J. 2008. Safety and efficacy of gene transfer for Leber's congenital amaurosis. *N Engl J Med* 358(21):2240–2248.
- Pinzon-Duarte G, Daly G, Li YN, Koch M, Brunken WJ. 2010. Defective formation of the inner limiting membrane in laminin beta2- and gamma3-null mice produces retinal dysplasia. *Invest Ophthalmol Vis Sci* 51(3):1773–1782.
- Sarig R, Mezger-Lallemand V, Gitelman I, Davis C, Fuchs O, Yaffe D, Nudel U. 1999. Targeted inactivation of Dp71, the major non-muscle product of the DMD gene: differential activity of the Dp71 promoter during development. *Hum Mol Genet* 8(1):1–10.
- Sene A, Tadayoni R, Pannicke T, Wurm A, El Mathari B, Benard R, Roux MJ, Yaffe D, Mornet D, Reichenbach A and others. 2009. Functional implication of Dp71 in osmoregulation and vascular permeability of the retina. *PLoS One* 4(10):e7329.
- Shen W, Fruttiger M, Zhu L, Chung SH, Barnett NL, Kirk JK, Lee S, Coorey NJ, Killingsworth M, Sherman LS, Gillies MC. 2012. Conditional Muller cell ablation causes independent neuronal and vascular pathologies in a novel transgenic model. *J Neurosci* 32(45):15715–15727.
- Tadayoni R, Rendon A, Soria-Jasso LE, Cisneros B. 2012. Dystrophin Dp71: the smallest but multifunctional product of the Duchenne muscular dystrophy gene. *Mol Neurobiol* 45(1):43–60.
- Yanoff M, Fine BS. 1996. *Ocular Pathology*. Mosby-Wolfe.
- Yin L, Greenberg K, Hunter JJ, Dalkara D, Kolstad KD, Masella BD, Wolfe R, Visel M, Stone D, Libby RT, Diloreto D Jr, Schaffer D, Flannery J, Williams DR, Merigan WH. 2011. Intravitreal injection of AAV2 transduces macaque inner retina. *Invest Ophthalmol Vis Sci* 52(5):2775–2783.